Neural Populations Can Induce Reliable Postsynaptic Currents without Observable Spike Rate Changes or Precise Spike Timing

Bryan Tripp[1] and Chris Eliasmith[1,2]

[1]Departments of Systems Design Engineering and [2]Philosophy, University of Waterloo, Waterloo, Ontario, Canada N2L 3G1

Fine temporal patterns of firing in much of the brain are highly irregular. In some circuits, the precise pattern of irregularity contains information beyond that contained in mean firing rates. However, the capacity of neural circuits to use this additional information for computational purposes is not well understood. Here we employ computational methods to show that an ensemble of neurons firing at a constant mean rate can induce arbitrarily chosen temporal current patterns in postsynaptic cells. If the presynaptic neurons fire with nearly uniform interspike intervals, then current patterns are sensitive to variations in spike timing. But irregular, Poisson-like firing can drive current patterns robustly, even if spike timing varies by tens of milliseconds from trial to trial. Notably, irregular firing patterns can drive useful patterns of current even if they are so variable that several hundred repeated experimental trials would be needed to distinguish them from random firing. Together, these results describe an unrestrictive set of conditions in which postsynaptic cells might exploit virtually any information contained in spike timing. We speculate as to how this capability may underlie an extension of population coding to the temporal domain.

Keywords: irregular firing, modeling, pattern generators, Poisson firing, temporal code, theoretical neuroscience

Introduction

Past theoretical and experimental work has shown how interneuronal communication through firing rates supports a wide range of computational processes. In some systems, additional information is contained in the precise timing of action potentials (e.g., Optican and Richmond 1987; Wright et al. 2002). Information–theoretical studies have extensively characterized the amount of information carried by action potential timing in sensory systems (e.g., Rieke et al. 1997). Although less widely studied, timing also appears to be important in motor and frontal areas (Abeles et al. 1993; Riehle et al. 1997). However, the functional relevance of information contained in spike timing depends entirely on what postsynaptic neurons can do with this information. This has motivated us to focus in this study on the effects that timing-based information can have on postsynaptic cells.

It is well-established that action potential timing plays a role in synaptic plasticity (see reviews by Kepecs et al. 2002; Dan and Poo 2004), but spike timing can also underlie computational processes. For example, activity in a neuron can depend on the degree of synchrony between the presynaptic neurons that converge onto it (Abeles 1982; Softky and Koch 1993; Singer 1999; Salinas and Sejnowski 2000). This phenomenon underlies perception of the horizontal location of low-frequency sound sources (Yin and Chan 1990; Brand et al. 2002) and has been suggested to play a significant role in high-level visual perception (although see Shadlen and Movshon 1999; Dakin and Bex 2002) and the recognition of odors (MacLeod et al. 1998; Brody and Hopfield 2003). Notably, synchrony-based computations can also be performed with asynchronously generated spikes, provided propagation times differ so that spikes arrive synchronously at their target (Hopfield 1995; Natschläger and Ruf 1998; Izhikevich 2006).

Less is known about how the timing of action potentials can affect computational processes in the absence of synchrony. But a number of cases demonstrate that the effects can be substantial. For example, information about tactile stimuli that are applied to human fingertips is encoded in the relative timing of the first spikes from different sensory neurons (Johansson and Birznieks 2004). This information can be extracted effectively by a projection with unequal excitatory synaptic weights and parallel inhibition (Thorpe et al. 2001). Similarly, information contained in the timing of consecutive spikes (in one neuron) can be extracted by certain types of synapses (Natschläger and Maass 2001), neurons (Segundo et al. 1963), or specific circuits (Ahissar 1998; Buonomano 2000; Knüsel et al. 2004). Also, some learning rules can lead simple neuron models to support a wide variety of mappings between incoming spike patterns and output (e.g., Legenstein et al. 2005; Gütig and Sompolinsky 2006). These examples illustrate that in a variety of situations, postsynaptic neurons may read out information contained in spike timing without relying on synchrony. However, the relevance of nonsynchronous spike timing to the operation of cortical circuits in general remains uncertain.

In particular, it is not yet clear whether nonspecialized neurons can use information encoded in arbitrary spike patterns in a flexible manner, that is, to compute arbitrary functions of the encoded signals. In this direction, Legenstein et al. (2005) have shown that spike timing–dependent plasticity can lead to input/output mappings that correspond to arbitrarily chosen sets of synaptic weights. However, this does not clarify whether mappings to arbitrarily chosen output spike patterns are possible. As we discuss below, the latter question has important implications for the interpretation of electrophysiological data. Therefore, we address here the question of whether there exist sets of synaptic weights that will transform arbitrarily selected patterns of spike timing into arbitrarily selected temporal patterns of current in a postsynaptic neuron model.

To answer this question, we use a conductance model to characterize synaptic currents, adjusting weights so that synaptically induced current at the soma optimally approximates preselected target patterns. We show that commonly observed types of firing patterns can drive a wide variety of current patterns in postsynaptic cells, regardless of whether their mean

rates vary over time. This remains true even if spike times vary randomly with a standard deviation (SD) of more than 10 ms. In some cases, effective postsynaptic currents (PSCs) can be driven by firing patterns that are so variable that the probability of distinguishing them from random firing is remote. Thus, in very general circumstances, the information contained in patterns of spike timing can be read out as arbitrary patterns of current in a postsynaptic cell. We conclude by suggesting how this phenomenon may underlie a versatile population–temporal coding scheme.

Materials and Methods

Simulations were performed using MATLAB® code that is available from the authors' web site (http://compneuro.uwaterloo.ca/).

Approximation of Current Patterns

The key procedure in this study is the assessment of how well given firing patterns can induce preselected patterns of current in a postsynaptic cell model. The target current was never induced exactly, but for a given presynaptic firing pattern, approximations of varying quality could be obtained by adjusting synaptic weights. We were interested in the best approximations that could be obtained for each firing pattern/target current pair.

Target currents were approximated by a linear combination of the PSCs that were induced at each synapse in a model cell. The optimal synaptic weights for approximating a given target current were found by adapting a method for decoding neural representations of scalars (Eliasmith and Anderson 2003). The following error function was minimized (using the Moore-Penrose pseudoinverse) with respect to synaptic weights w:

$$E = \int^T [I(t) - \sum w_i I_i(t)]^2 dt$$

where E = error, $I(t)$ is the current pattern to be approximated, w_i is the weight of the ith synapse, I_i is the unweighted PSC pattern at each synapse, and t is time. In cases where firing patterns varied from trial to trial due to noise, the above integral was evaluated over 32 repeated trials to find optimal weights, and performance was then evaluated as the average mean-squared error (MSE) over 5 additional trials. Accuracy improved with greater numbers of trials but improved little with 64 as opposed to 32 trials.

The model of current dynamics at each synapse was adapted from a model of alpha-amino-3-hydroxy-5-methyl-4-isoxazoleproprionic acid receptors (Destexhe et al. 1998). This model determined the temporal shape of the current at each synapse, whereas the optimal synaptic weights determined the absolute scale. The results of this study were not sensitive to alternate PSC models, different time constants of current decay, or diverse time constants at different synapses. We adopted the common simplifying assumption that synaptic currents combine linearly at the soma (e.g., Gütig and Sompolinsky 2006; Izhikevich 2006). This is a reasonable approximation of some, but certainly not all, cases of synaptic integration, depending on factors such as intrinsic currents and the spatial distribution of synapses (e.g., Poirazi et al. 2003). Linear combination was achieved by holding membrane potential (at the synapse) at –65 mV, a constant far from the reversal potential. By summing conductances instead of currents, the analysis can be generalized to any case in which there is a monotonic relationship between conductance and current, but this additional complexity is avoided here.

We focused on target current patterns in the 0- to 5-Hz band, which approximates the range of frequencies over which neural firing rates change in many circuits. For example, muscle activation patterns in humans (which are rate coded) consist mainly of frequencies under 5 Hz. A selection of band-limited target currents was generated by assigning random coefficients to different frequency components and calculating the inverse fast Fourier transforms.

Presynaptic Firing Patterns

Presynaptic firing patterns were obtained in 2 different ways. First, an initial study was performed with firing patterns produced by a cortical

network model. Second, synthetic spike trains with desired statistical features were generated by drawing interspike intervals (ISIs) from appropriate probability distributions. These methods are described in detail below.

Network Simulation

The cortical network model (Izhikevich 2003) consisted of 200 fast-spiking inhibitory and 800 excitatory neurons, the latter mainly adapting with some bursting neurons. In some simulations, the coefficient of variation (CV; i.e., the SD divided by the mean) of ISIs (within the spike train of each neuron) was increased. CV was increased by shifting the excitatory neuron distribution to favor bursting neurons and decreasing excitatory coupling by 40%.

Synthetic Spike Trains

Synthetic spike trains were used to explore in detail how the results obtained from the cortical network model related to its patterns of firing. ISIs for synthetic spike trains were drawn from 3 types of probability distributions: Gaussian centered on a mean firing rate (repetitive spiking), a shifted exponential distribution with zero probability between 0 and 2 ms (Poisson-like pattern with refractory period) and a bimodal distribution consisting of the sum of 2 Gaussians, chosen so as to obtain a specified mean rate and CV = 2 (irregular bursting). To obtain spike trains with CV < 1, the Gaussian and exponential distributions were combined in a weighted average. Spike trains with CV between 1 and 2 were obtained by averaging the exponential and bimodal distributions.

Because each synthetic firing pattern was generated from a single ISI distribution, we refer to these patterns as having constant firing rates. Because the mean rates do not change over time, ISI ordering makes up all the information content of these firing patterns. This means that, for example, the Poisson patterns in this study are not treated as Poisson noise, but as information with Poisson statistics. Noise was introduced separately, either as spike time jitter or in the form of additional spikes that were introduced at random from trial to trial.

It was hypothesized that firing time correlations across different neurons might also affect performance, separately from the effects of the temporal regularity of firing patterns. Spike trains with different levels of pairwise correlation were produced in 2 ways.

Method A. Spikes were distributed in a Gaussian pattern (SD = 3 ms) around Poisson-distributed correlation times (Benucci et al. 2004). The degree of correlation was varied by changing the rate of correlation times relative to the firing rate. For example, when the rates were similar, each spike train contained a spike at almost every correlation time, and pairwise correlations were very high. Correlations were low when the firing rate was much lower than the rate of correlation times.

Method B. Poisson firing rates R in each spike train were varied over time according to the template function: $R = A\max(0, \sin(2\pi Bt) - C)$, where B = 10, 22, or 55 Hz, t is time, C is a threshold between –2.0 and 0.9, and A is a constant that normalizes the template to produce the desired mean firing rate. At higher thresholds, firing only occurred at peaks of the sine wave, resulting in high correlations.

As an index of pairwise correlation, we report the peak cross correlation $R = (R_{AB} - N_A N_B / N) / [(N_A - N_A^2 / N)(N_B - N_B^2 / N)]^{1/2}$, where R_{AB} is the number of coincidences in each 1-ms bin, N_A and N_B are the numbers of times that cells A and B fire, and N is the number of bins (e.g., Tomita and Eggermont 2005). These methods result in similar degrees of correlation between different pairs in an ensemble. This is a simplification, in that there is typically substantial variation between pairwise correlations in a real neural ensemble.

Statistical Power Analyses

Statistical power analyses were performed in order to determine the numbers of experimental trials that would be needed to detect the subtlest firing patterns that could drive reproducible activity in postsynaptic targets (see details in Appendix). These analyses apply to experiments that consist of repeated recordings of a single excitatory cell from a population with Poisson firing statistics. Cells that are

postsynaptic to this population may also receive inputs from other populations, but the net effect of other inputs is assumed to be nearly constant.

Results

Cortical Network Simulation

A simulated network of 1000 irregularly firing cortical neurons (Izhikevich 2003) was able to generate PSCs that closely approximated a wide variety of target patterns. Figure 1 shows current patterns generated simultaneously by this network in 3 different postsynaptic cell models, which differ only in terms of synaptic weights. The current pattern in the first cell is a smoothed and scaled version of the network's mean firing rate. This is the type of current pattern that would emerge with uniform or random synaptic weights, so it is not surprising that this target pattern can be approximated very closely when synaptic weights are optimized specifically for this purpose. The current pattern in the second cell is an arbitrarily chosen square pulse. In contrast with the current pattern of the first cell, this current pattern is not related to the network's firing rate or to any other time-varying statistic of the network's activity. However, with appropriately chosen synaptic weights, this pattern is also approximated accurately. The current pattern in the third cell consists of randomly selected frequency components in the 0- to 5-Hz band. Like the square pulse, it bears no obvious relationship with the network's firing pattern, but it is also well approximated. Somatic current in each of these cells deviates less than 1% from the target, in the mean-squared sense. These examples show that a given pattern of firing may drive an extremely wide variety of PSCs given appropriately chosen synaptic weights.

Firing Pattern Regularity

This basic result does not address how statistical features of a population firing pattern might constrain the current that it can induce in a postsynaptic cell. Synthetic spike trains were used to explore this question in detail. Approximation error was found to depend strongly on the regularity of spike trains over time. Figure 2 (panels A–D) shows approximations of band-limited current patterns by firing patterns with differing temporal regularity. Notably, spike trains with essentially constant firing rates (e.g., Fig. 2A,B) could approximate arbitrarily chosen time-varying current patterns in the postsynaptic cell model. However, error was markedly reduced as the CV of ISIs increased.

These results are not surprising when the currents at individual synapses are considered in the frequency domain. The currents at individual synapses can be viewed as temporal basis functions, which are weighted and summed to approximate the target pattern. The frequency content of these basis functions depends on the firing pattern of the corresponding presynaptic cell. For example, the current that arises from regular firing consists of harmonics of the firing frequency, whereas that arising from Poisson firing has a broad spectrum. This can be seen in the lower traces of Figure 2A–D, which show the power spectra of the first several principal components of the PSCs that are induced by each ensemble. Approximation error decreases with increasing power in the frequency range of the target current and increases with increasing power at other frequencies.
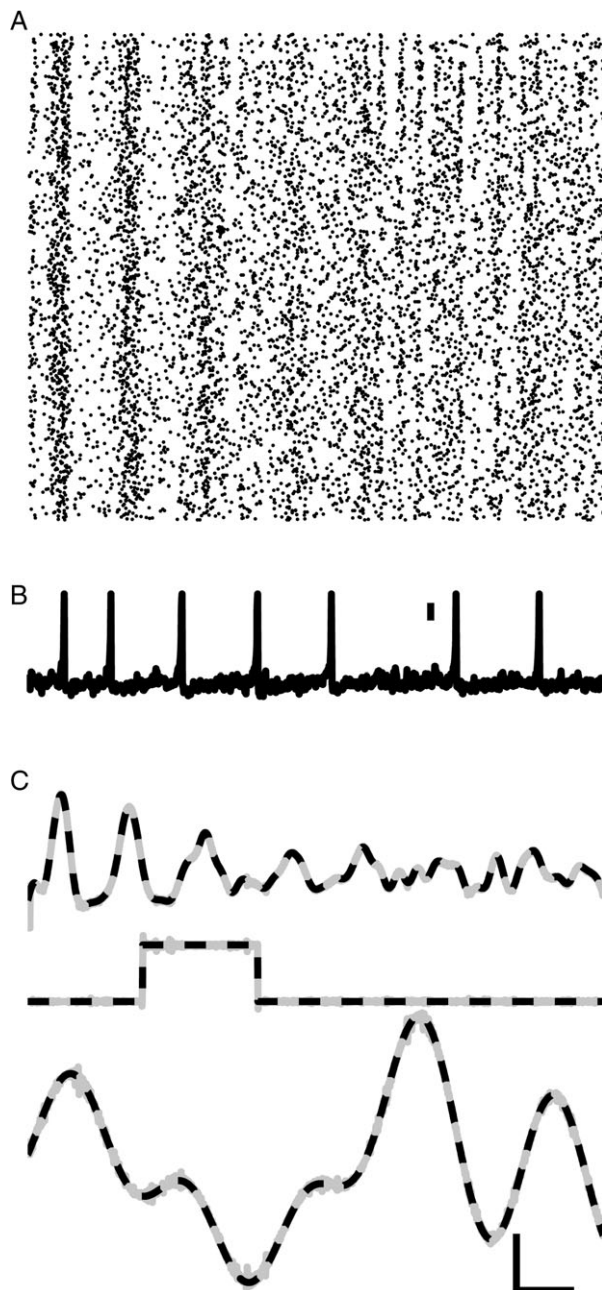

Figure 1. Pattern generation example. A model of 1000 cortical neurons (Izhikevich 2003) can generate arbitrarily chosen current patterns in a postsynaptic cell. (A) Spike times (one neuron per row). (B) Membrane potential of a typical excitatory neuron in this network (scale bar 20 mV). (C) Current induced in 3 different postsynaptic cells, to which the network projects with different synaptic weights. Currents are optimal approximations (gray) of target patterns (black dashed). Top: smoothed and scaled reflection of the network's mean firing rate, middle: an arbitrarily chosen square current pulse, bottom: an arbitrarily chosen band-limited target (scale bars: 1 nA and 100 ms). Timescale in (C) applies to all panels.

As a result, both Poisson-refractory and irregular-burst firing patterns can accurately generate target currents with a wide range of frequencies. Burst firing is more effective than Poisson-refractory firing for driving low-frequency current patterns. However, Poisson-refractory firing is effective over a slightly wider frequency range (Fig. 2E). Firing patterns in most neural circuits tend to have high CV. These results begin to suggest
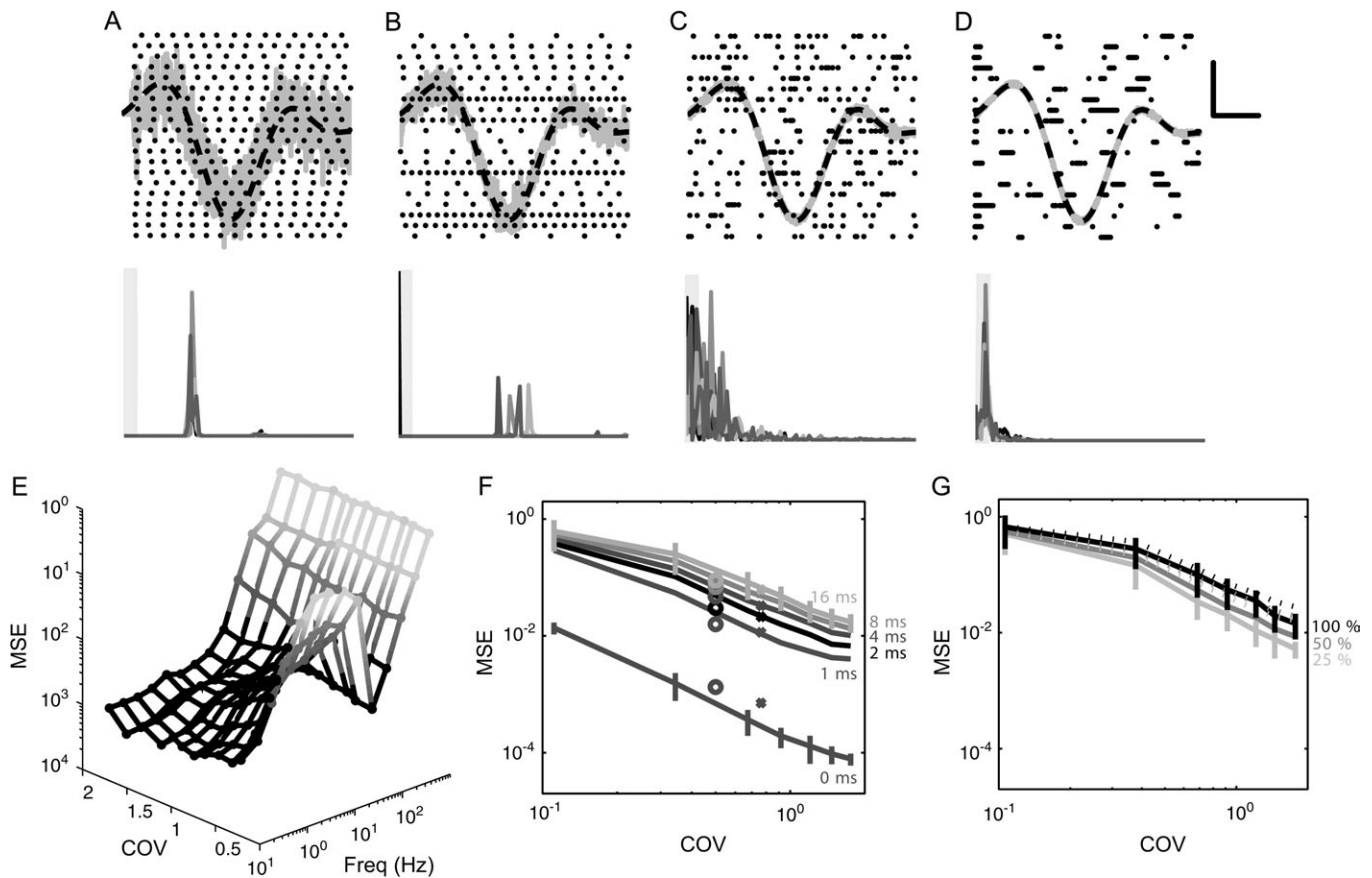
Figure 2. Decreasing error with decreasing spike pattern regularity. All data are from simulations with 500 synthetic neurons, with mean firing rate 30 Hz, but different ISI distributions. In panels (A–D), dots represent spike times of example neurons, black dashed lines are target currents, and gray lines are actual net synaptic currents flowing into the postsynaptic cell model. Traces below are power spectra of the first 5 principal components of the PSCs (range 0–100 Hz; shaded area 0–5 Hz). (A) Neurons that fire at near-constant rates (CV = 0.08; MSE = 0.117 nA). (B) Constant rates with wider rate distribution (across neurons) than in (A) (CV = 0; MSE = 0.015 nA). (C) Poisson-refractory neurons (CV = 0.94; MSE = 0.002 nA). (D) Irregular-bursting neurons (CV = 1.7; MSE = 0.0003 nA). (E) MSE (as a proportion of root-mean-squared target current amplitude) in approximating sinusoids of different frequencies (mean over 5 different phases at each frequency) for a wide range of CV. Error is generally high with low CV, except when sinusoid frequency is close to the mean firing frequency. (F) MSE versus CV. Separate lines are degrees of Gaussian jitter (SD as labeled). Error bars on top and bottom traces indicate SD over 5 randomly selected band-limited signals. Symbols O and X indicate means for a 500-neuron version of cortical network and for the same network adjusted for higher CV (see Materials and Methods), respectively. (G) As (F) but with noise in the form of additional, randomly timed spikes instead of jitter. Number of noise spikes given as percentage of number of nonnoise spikes. Dashed lines of the same shade indicate errors with the same proportion of noise spikes plus 4-ms jitter.

that information contained in such patterns can be extracted in an accurate and flexible manner.

Spike Jitter and Noise Spikes

The results described so far are highly idealized in that they are based on noise-free firing patterns. In order to quantify the dependence of current generation accuracy on precise spike timing, simulations with synthetic spike trains of different CV were repeated with random (Gaussian distributed) spike time jitter.

Spike jitter with a given variance had the effect of increasing MSE by a near-constant multiple, regardless of CV. Thus at high CV, where error without spike jitter was minimal, error remained relatively low even when substantial jitter was applied. For example, with bursting spike trains (CV > 1), 8-ms jitter resulted in error of at most 5% of root-mean-squared current (Fig. 2F). Similar results were obtained when firing patterns were corrupted by inserting additional "noise spikes," at random times (determined by a constant-rate Poisson-refractory process) that were uncorrelated between repeated trials (Fig. 2G).

Figure 3 shows an example in which half of the spikes are noise spikes and the other half are subject to extreme Gaussian jitter (σ = 20 ms). The target pattern is nevertheless approximated with reasonable accuracy, illustrating that meaningful population output requires very little consistency in the fine temporal firing patterns of individual neurons, even in the absence of coarse firing rate variations.

Population Size and Firing Rate

For firing patterns with a given CV, error decreased with increasing presynaptic population size (Fig. 4). However, very large populations were not needed. For example, with 1-ms spike jitter, 1000 presynaptic Poisson-refractory neurons were adequate to generate 500-ms signals with roughly 2% MSE.

In contrast with population size, firing rate had little effect on the accuracy of current generation. Errors arising from Poisson-refractory inputs were consistent over a wide range of intermediate firing rates, increasing slightly both below 5 spikes/s and above 100 spikes/s (Fig. 5). The increase in error with higher rates is related to the fact that the refractory time causes a more pronounced deviation from Poisson statistics (lower CV)
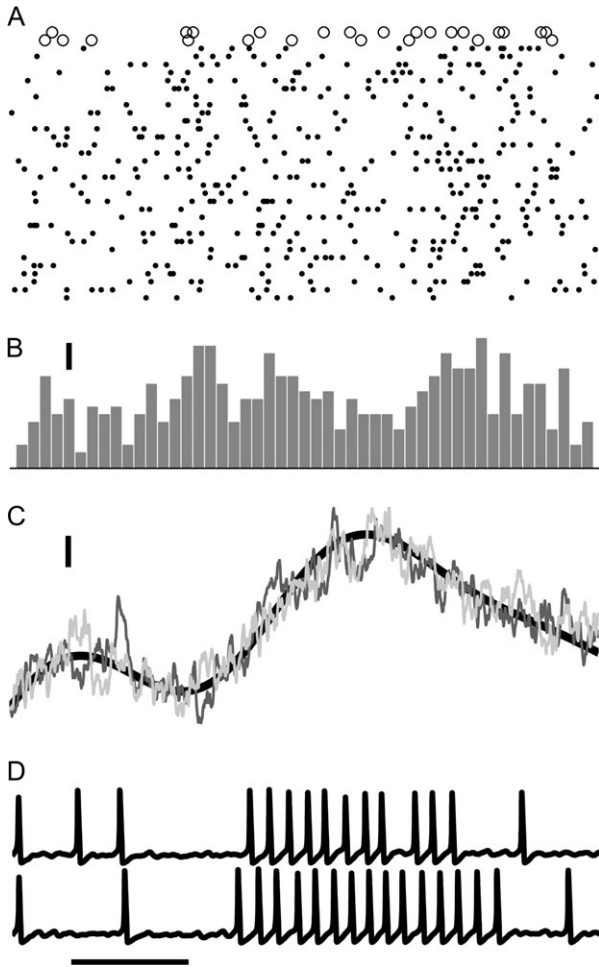
Figure 3. Moderate error with highly variable spike trains. The presynaptic population consists of 1500 synthetic Poisson-refractory spike trains. Each train consists of 2 interlaced 20 spike/s components. One component is subjected to large spike jitter (SD = 20 ms) that is uncorrelated between trials. The other component is completely uncorrelated between trials (i.e., in each trial, this component consists of a new set of spikes from a Poisson-refractory process, which is independent of previous sets). (*A*) Spike times of an example presynaptic neuron, over 32 trials used to find synaptic weights (dots), and 2 separate trials shown in panel (*C*) (circles). (*B*) Spike time histogram of a single example neuron (scale bar: 10 spikes/s). (*C*) Approximations (gray) of target current (black) for the 2 trials shown as circles in (*A*) (scale bar: 2 nA). (*D*) Membrane potential of a Hodgkin–Huxley model (Koch 1999) driven by the 2 current approximations shown in (*C*) (scale bar: 100 ms applies to all panels).

Figure 4. Error decreases with increasing population size. Results from Poisson-refractory neurons (40 spikes/s), with different degrees of Gaussian spike time jitter are shown (jitter SD as labeled). Error bars on top and bottom traces indicate mean ± SD of MSE over 5 randomly selected band-limited target currents (as a proportion of root-mean-squared target current amplitude). Error varies with spike jitter as in Figure 2.

Figure 5. Error is nearly constant over a broad range of firing rates. Separate lines correspond to Gaussian jitter with SD as labeled. Solid black: Poisson-refractory neurons. Dashed gray: Poisson neurons. Error bars on top and bottom traces indicate mean ± SD of MSE over 5 randomly selected band-limited target currents (as a proportion of root-mean-squared target current amplitude).

at higher rates. This can be seen by comparing the solid and dashed lines in Figure 5.

Correlated Firing

We have essentially characterized synaptic currents as having low-frequency components that form an overcomplete temporal basis of possible somatic currents, over some range of frequency and time. Because such functions span a larger space if they are linearly independent, we hypothesized that spike timing correlations would impair performance. Synthetic spike trains were used to test this prediction (note that we did not study correlated variability here, as others have done, e.g., Abbott and Dayan 1999; Schneidman et al. 2003). Error generally increased with correlated spike timing because when spikes were concentrated around correlation times, there were fewer spikes in the intervening periods, which is analogous to the
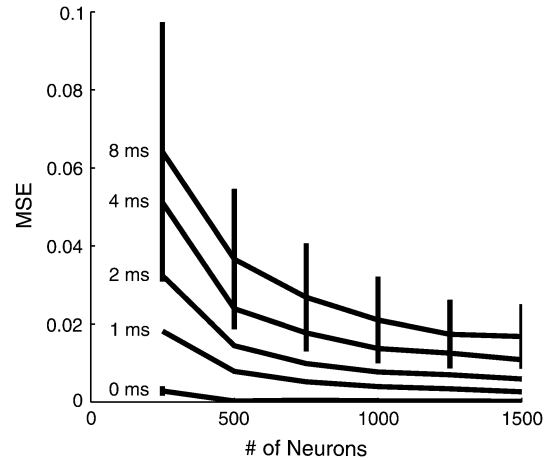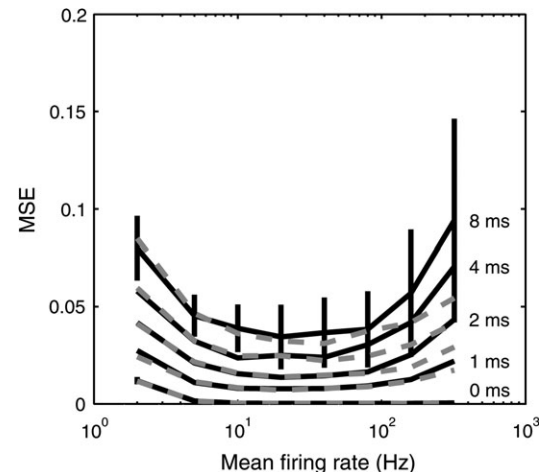
population briefly consisting of fewer neurons (see previous section). However, the increase in error was minimal when correlation times were periodic at high frequencies (Fig. 6). This can be explained by noting that when correlation times are frequent, some of the PSCs that begin flowing around one correlation time will continue to flow until the next, so that the effective population size remains large throughout. These results suggest that although correlated firing may underlie some forms of temporal coding, it may preclude other forms that rely on diverse timing to support a wide range of temporal transformations. Another possibility is that correlated firing may gate such codes dynamically.

Learning

The results presented above are based on synaptic weights that were obtained using an artificial optimization method. The physiological relevance of these results depends on whether
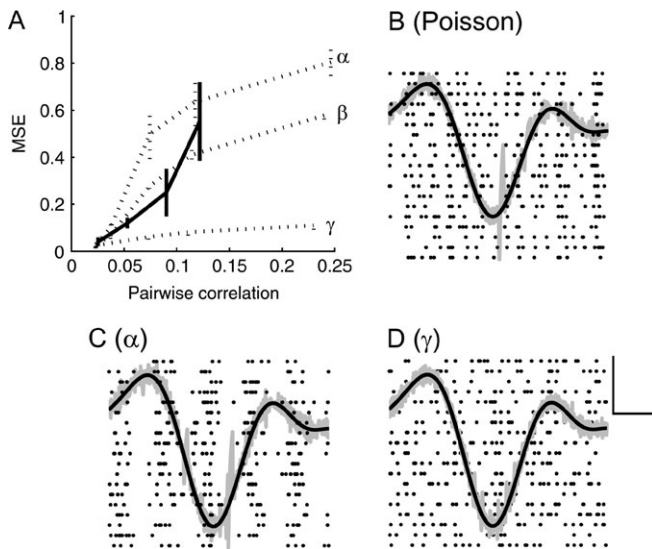
Figure 6. Increasing error with increasing spike time correlation. (*A*) MSE versus correlation (4-ms jitter) with 500 Poisson-refractory neurons (40 spikes/s). Solid and dashed lines indicate Poisson and periodic correlation times, respectively (see Materials and Methods; $\alpha = 10$ Hz; $\beta = 22$ Hz; $\gamma = 55$ Hz). MSE reported as proportion of root-mean-squared target current amplitude; bars indicate SD over five 300-ms targets. (*B–D*) Examples of approximations with Poisson, α, and γ correlations of roughly equal strength. Dots represent spike times of example neurons, black lines are target currents, and gray lines are the actual synaptic currents flowing into the postsynaptic cell model. Scale bars: 100 ms and 1 nA.

each synaptic weight can be independently learned, using only information that is available at the corresponding synapse. We found that synaptic weights can indeed be learned in this manner, provided some explicit error or target signal is available.

The derivative of the error function defined earlier (see Materials and Methods), with respect to each synaptic weight, equals the inner product of the current and the error over time. This suggests a supervised learning rule in which each synaptic weight is updated at each instant, by $\Delta w_i = -\kappa I_i^{\mathrm{syn}} E$, where κ is a constant learning rate, I_i^{syn} is the instantaneous current at the i synapse, and E is the instantaneous error in net current. This learning rule quickly converges on results similar to those obtained with the optimization method (Fig. 7). This remains true in the presence of spike jitter.

Assuming an error signal were available, it is doubtful whether this signal would propagate instantly to each synapse. We therefore investigated the performance of the learning rule when Δw_i was based on low-pass filtered error and current signals. Filtering obscured high-frequency errors from the learning mechanism. Consequently, learning was slowed, and the resulting approximations contained more noise in the frequency range corresponding to the stop band of the filter (Fig. 7). However, these limitations were not severe. Reasonable approximations were obtained even when the filter time constant was greater than the duration of the target signal. This demonstrates that learning can proceed on the basis of error information that is substantially lagged and temporally smoothed.

Experimental Detection of Subtle Repeated Patterns

As previously demonstrated, spike patterns with little trial-to-trial consistency can drive highly consistent activity in a postsynaptic target (Fig. 3). This raises the question of whether spike patterns that have a stereotyped relationship with behavior might be driven by spike patterns that are so variable
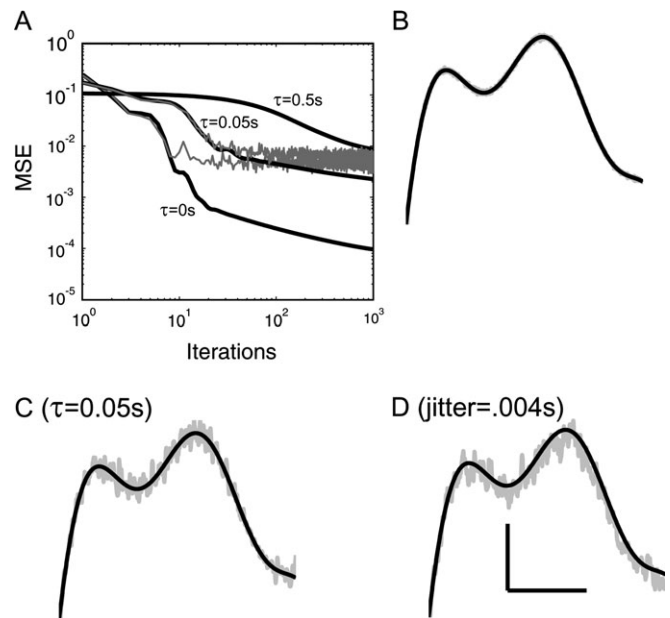

Figure 7. Learning. (*A*) Decrease in error over 1000 iterations of a Poisson-refractory spike pattern (500 neurons; 30 spikes/s), under the learning rule described in the text (see Results under the heading "Learning"). All synaptic weights initially set to zero; target current as shown in other panels. Thick black lines indicate learning trials with no spike jitter. Three cases are shown, each with error data temporally filtered using a different first-order low-pass filter (time constants as labeled; $\tau = 0$ indicates no filter). The thin gray lines that diverge from the black lines after ~10 iterations indicate corresponding cases repeated with 4 ms (SD) jitter in the spike trains (only the $\tau = 0$ s and $\tau = 0.05$ s cases are shown). Interestingly, there were substantial differences in error after a single iteration (left extreme of each line), depending on the filter time constant. Substantial filtering allowed the learning mechanism to accurately approximate the mean magnitude of the target signal in a single pass, although subsequent learning of the signal shape was slowed. Learning continued after 1000 iterations (not shown). For example, with $\tau = 0.5$, error was further reduced by about half, after 10 000 as opposed to 1000 iterations. Panels (*B–D*) show target current (black) and approximation (gray) in various cases, after 1000 iterations. (*B*) Neither filter nor spike jitter. (*C*) Filter with $\tau = 0.05$ s. (*D*) Spike jitter with SD = 4 ms. Scale bars: 100 ms and 0.5 nA.

with respect to behavior that any underlying consistency evades experimental detection. Statistical power analyses were performed to address this question. The analyses estimate the numbers of repeated trials that would be needed to find perievent variations in firing rate, under the assumption that such variations are as small as possible while still producing relatively reliable spiking in a postsynaptic cell.

Figure 8 shows the numbers of trials that would be needed to detect the subtlest presynaptic firing patterns that could drive postsynaptic firing with various levels of consistency. The number of trials needed depends strongly on how reliable postsynaptic spiking is assumed to be. This is because the more pronounced variations in presynaptic firing that would be needed to cause more reliable postsynaptic firing would also require fewer trials to detect. However, even if postsynaptic spiking were highly stereotyped (1% of spikes timed inconsistently from trial to trial), 50 or more repeated trials may be needed to distinguish the driving patterns from random firing. Throughout the range of error rates shown in Figure 8*A*, trial-to-trial consistency is greater in postsynaptic than in presynaptic firing patterns. So, presynaptic firing patterns that are so subtle as to require over 1000 trials to detect may nevertheless drive much more stereotyped activity in postsynaptic cells. Although
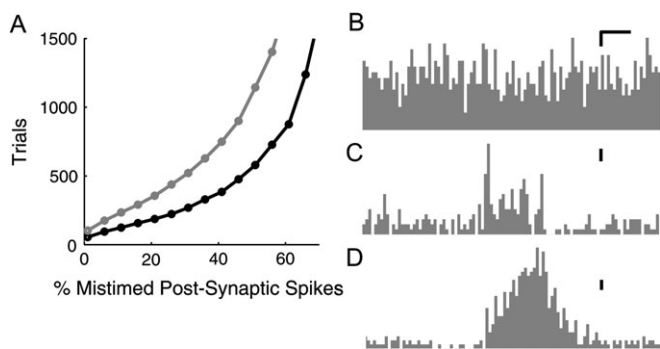
Figure 8. Trials needed to detect subtle firing patterns. Results of prospective power analyses for (hypothetical) experiments to detect the smallest perievent firing rate changes that could trigger reliably timed spiking in a postsynaptic cell. Assumptions are as described in Materials and Methods. Details of the analysis are given in the Appendix. (*A*) numbers of trials required for a type-II error rate of 0.2 with 1-way ANOVA. More trials are needed to detect smaller presynaptic fluctuations in firing rate. The expected size of presynaptic rate fluctuations depends on the number of neurons contributing to each postsynaptic spike (black: 500; gray: 1000) out of a total of 10 000, and on the reliability with which the postsynaptic cell is assumed to spike. For example, larger presynaptic variations in firing rate lead to more reliable postsynaptic timing and also require fewer trials to detect. An impractically large number of trials may be needed to detect subtle patterns, unless it can be assumed that the patterns drive postsynaptic activity with a very low error rate. (*B*) 100-trial spike timing histogram for an example neuron drawn from a population that drives postsynaptic firing with a mistimed spike rate of ~60%. (*C*) 100-trial firing histogram for a Hodgkin–Huxley neuron driven by the population exemplified in (*B*) with PSC time constant of 5 ms. (*D*) As (*C*) but with 20 ms PSC time constant.

the specific results of this analysis clearly depend on the assumptions made (e.g., degree of convergence; Poisson firing statistics), we take it that the same or similar assumptions describe many cortical and subcortical areas. The key observation is that substantially more trials may be needed to detect useful repeated firing patterns (e.g., over 100 trials, if a 10% rate of postsynaptic spike mistiming is assumed) than are typically collected in experimental studies (except in studies in which repeated trials consist only of brief sensory stimuli, e.g., Bair and Koch 1996).

In fact, these results may underestimate the capacity for highly variable spiking to produce stereotyped behavior because the power analyses ignore potential dynamic effects. Specifically, firing at the output of a network will have greater consistency if the network is more responsive to underlying firing patterns than to random fluctuations. Figure 8*D* shows the results of a simulation that illustrates this point using a Hodgkin–Huxley model (Koch 1999) of a postsynaptic neuron. In this simulation, the receiving neuron is made less responsive to high-frequency random fluctuations in excitation, simply by including PSC dynamics with a relatively long time constant of 20 ms. Depending on the frequency content of signals in a given circuit, this particular filtering mechanism might not be useful. However, there are other more sophisticated neural circuits that can perform, for example, band-pass filtering with any choice of corner frequencies (Tripp and Eliasmith 2006). This reinforces the conclusion that precise, reproducible behavior can in theory arise from highly variable neural activity.

Discussion

We have shown that even in the absence of coarse rate variations, irregular firing patterns can drive nearly any given pattern of activity in a postsynaptic neuron. Importantly, such

transformations can be obtained through learning. These results have 2 main implications in terms of the interpretation of experimental data. First, a neuron's pattern of firing around an event may not have an obvious temporal relationship with the neuron's role in the event. For example, although a group of neurons fires faster only at the end of a movement, subtle differences in spike timing between neurons may drive some aspect of movement initiation. This is particularly true with respect to irregular and highly stereotyped firing patterns, such as those arising in middle temporal responses to some visual stimuli (Bair and Koch 1996) or in songbird vocalization (Hahnloser et al. 2002; although the same cannot be said if responses lack diversity across the population, e.g., see Reinagel and Reid 2002). Furthermore, accuracy degrades gracefully with firing pattern variability, so that even firing patterns that are difficult to distinguish from random firing can drive relatively stereotyped activity. Therefore, the second main conclusion to be drawn from this study is that neither precise spike timing nor observable rate fluctuations can be relied on to expose all the significance of a cell's activity.

Although we have studied projections from a single neural ensemble to a single postsynaptic neuron, the results also have implications for larger circuits. A single ensemble of neurons can drive different postsynaptic neurons in entirely different patterns (e.g., Fig. 1*C*). As we have shown, several hundred neurons driven in diverse patterns would form a rich basis from which to drive activity in a subsequent layer. Therefore, although it remains to study how errors propagate through multiple layers, the present results clearly apply to larger circuits as well as to single projections.

Our findings are in general agreement with the results of Gütig and Sompolinsky (2006) on the classification of firing patterns. If a neuron can be trained to spike in response only to selected population–temporal input patterns, as they have shown, then it would be expected that the same neuron could be made to exhibit arbitrarily chosen firing patterns by training it to respond only to selected short segments of a longer presynaptic pattern.

Medina et al. (2000) present a model of a specific neural circuit that they take to function in similar manner to the abstract circuits in the present study. Theirs is a classical conditioning model, in which cerebellar granular cells respond to a conditioned stimulus with diverse temporal firing patterns. An unconditioned stimulus serves as a training signal, decreasing or increasing the strength of granular cell synapses onto Purkinje cells, depending on whether granular cell activity is coincident with the unconditioned stimulus or not. After training, Purkinje cells in effect decode a temporal prediction of the unconditioned stimulus from diverse granule cell firing patterns. Synaptic weights are modulated on the basis of a target output rather than error, so learning ends when some physiological parameter is saturated, rather than when error is minimized. Otherwise, this learning mechanism is analogous to the one presented here.

The present study is also conceptually related to the liquid-state machine (Maass et al. 2002). The liquid-state machine relies on a diversity of neural responses to input, within a recurrent circuit, in order to approximate a broad class of temporal functions of the input. In contrast to the liquid-state machine (the neurons of which fire at fluctuating rates), the present study explores how computations are effected by firing statistics in the absence of large-scale rate fluctuations. This

focus leads to new implications (as describe above) with respect to the interpretation of electrophysiological data.

Effects of Firing Statistics on Performance

The relationships between the statistics of presynaptic firing patterns and the accuracy of PSC generation are remarkable in several respects. First, we have demonstrated that the irregularity of experimentally observed spike trains can provide a substantial functional advantage in terms of 1) the accuracy with which neurons can drive current in a postsynaptic cell and 2) the robustness of the current pattern to noise. For slowly varying current patterns, this advantage is even more pronounced with bursting neurons, highlighting a possible dimension in the functional relevance of burst firing that has received little attention (e.g., in Crick 1984; DeBusk et al. 1997; Lisman 1997; Reinagel et al. 1999; Izhikevich et al. 2003; Kepecs and Lisman 2003).

Second, although it is well-established that greater numbers of neurons can drive current more accurately, we have demonstrated that even in the absence of precise spike timing or rate variations, very large numbers of neurons are not needed. As shown in Figure 3, 1500 irregularly and inconsistently firing neurons can drive useful PSC patterns. The degree of convergence onto most neurons is far greater than this. For example, some α-motoneurons receive about 50 000 synaptic inputs, and cerebellar Purkinje cells receive as many as 200 000. This indicates that multiple firing-rate–independent signals could converge on a single neuron pool. Furthermore, the same population firing pattern can induce vastly different currents in different cells (e.g., Fig. 1C), so the same small group of neurons could drive a wide variety of activity elsewhere, limited only by the number of different cells to which it projects.

Third, we have noted that under the conditions studied here, errors in PSC are greater when the timing of presynaptic spikes is correlated. However, we have also shown that the increase in error is moderate when spike times are correlated at high frequencies. It is interesting to consider this result in relation to oscillations in local field potential (LFP), particularly in the context of motor control. Lower frequency alpha and beta oscillations in motor cortical LFP usually disappear during movement and are sometimes replaced, around movement onset, by higher frequency gamma oscillations (MacKay 1997). Similar changes in LFP oscillations during movement occur in the cerebellum (Pellerin and Lamarre 1997) and basal ganglia (Cassidy et al. 2002; Levy et al. 2002; Courtemanche et al. 2003; Kühn et al. 2004). Thus, patterns of LFP oscillation in motor areas during movement and rest coincide with patterns of synchrony that allow and preclude (respectively) the type of coding presented here, pointing to the possibility of a role for this type of coding in motor control.

Fourth, and finally, we have shown that errors in pattern generation were dominated by high-frequency fluctuations, a point that is also relevant to motor control. For example, 75% of the error in Figure 2A was at frequencies above 100 Hz, much higher than the frequency content of skeletal movement. The frequency spectrum of the error is relevant in the context of motor control because the relationship between myoelectric activity and muscle forces resembles a low-pass filter (Olney and Winter 1985), and limb inertia has a further damping effect. Thus, most of the error observed in this study (i.e., error at high

frequencies) would not necessarily interfere with movement kinetics if it were present in a motor circuit.

Timing versus Rate

Each of the synthetic firing patterns used in this study was generated from a constant ISI distribution and in this sense has a constant mean firing rate. However, instantaneous rates fluctuated because the patterns (with the exception of those in Fig. 2B) contained a range of ISIs. So, if these firing patterns were repeated over multiple trials, rate fluctuations would appear in the multitrial spike histogram (although such fluctuations might be quite subtle, as in Figs 3 and 8). However, repeated task behavior does not guarantee that related neurons exhibit repeated patterns. For example, a neuron's activity may reflect something that varies from trial to trial, such as an error signal. Also, a neuron's firing pattern might contain information about a repeated feature of an event only when considered in conjunction with the firing patterns of other neurons (Schneidman et al. 2003). For example, there are nearly identical segments in the final 2 rising slopes of the bottom trace of Figure 1C; one is coincident with a gamma oscillation and the other is not. Because instantaneous rate does not uniquely determine multitrial rate, even if the neuron is noise free, and because it is otherwise indistinguishable from timing, we use the term "rate" only to indicate the inverse of the mean of the ISI distribution.

Limitations and Future Work

The most important limitation of this study is that the dendritic model used here assumes linear combination of currents, as might occur, for example, with synapses on separate distal dendrites (Poirazi et al. 2003). Dendrites can also combine synaptic input in much more complex and varied ways, although some complexities of dendritic processing (including dendritic spiking) serve partly to compensate for passive cable properties rather than to implement nonlinear computations (Magee 1999; Magee and Cook 2000; Williams and Stuart 2000; Rudolph and Destexhe 2003). As noted in Materials and Methods, the present results are relevant to any case in which PSC is a monotonic function of total conductance. For any target current, in such cases, there is a corresponding sum of conductances that will produce it. In more complex cases, the present results may only apply under limited conditions, for example, to activity within a single dendritic branch or within a certain voltage range. It is beyond the present scope to explore how these results interact with more detailed models of specific cell types, but we expect that in many cases, sophisticated dendritic processing would enable further computations on the results of the computations modeled here. For example, several temporal current patterns that are generated by near-linear synaptic integration might converge to be combined multiplicatively. The possibility of such additional dendritic processing does not seem to affect the basic conclusion that arbitrary timing-based information can be exploited in a flexible manner, under very general circumstances.

One aspect of dendritic processing that would be particularly interesting to study, in relation to the current results, is variability in the dendritic membrane time constant (e.g., through neuromodulation). Changes in membrane time constant would alter the temporal relationships between somatic currents arising from different parts of the dendritic tree. If weights were tuned in relation to one time constant, such

changes would be expected to result in additional noise in the somatic current, at frequencies of about 50 Hz and higher. However, it might be possible to tune synaptic weights in order to exploit such changes functionally. For example, modulation of the time constant might synchronize or desynchronize distal excitatory inputs from more proximal inhibitory inputs, dramatically influencing the spiking pattern.

We have shown that in principle, timing patterns can be exploited by the brain even if they are difficult to detect experimentally. This result is in a sense its own limitation, because it would be difficult to confirm that this was actually happening in a given circuit. A prerequisite would be that some functionality of a circuit could not be accounted for by firing rates or precise timing. Specific results of this study (e.g., relationships between error and firing statistics) may also help to resolve whether such a mechanism is feasible given other knowledge of the circuit. However, the only obvious way to test for this phenomenon directly is to perform large numbers of trials.

Another limitation of this study is that although we have identified a learning rule that makes use of information that could plausibly be available at each synapse (i.e., each synapse does not need information from other synapses), this rule is speculative rather than being based on a known biological mechanism. It remains either to map this learning rule onto a demonstrated mechanism or to explore the viability of other rules, for example, rules based on rewards rather than error signals.

Although we have focused on how an ensemble of neurons can produce a single pattern of PSC in a given cell, it is unlikely that a cell is dedicated to producing a particular pattern. As a result, further work is needed to explore how our results generalize to the production of different current patterns in the same cell over short timescales, that is, without substantial changes in synaptic weights. There are several possibilities. For example, an ensemble could produce a family of pattern primitives, which could be separately gated to produce a wide range of PSC patterns. A circuit of this form might function as a repository of arbitrarily complex motor programs, with parameters varied through gating.

It may also be fruitful to explore how the firing patterns that arise from varying input to a network could drive a useful set of outputs. Certainly, the firing patterns that are produced by 2 different inputs could produce essentially any 2 patterns of PSC. This is clear if one imagines that the spike pattern from 0 to 500 ms in Figure 1 is produced by one input and the pattern from 500 to 1000 ms is produced by a second input. With a single set of synaptic weights, the 2 inputs result in 2 different current patterns. This remains true for more than 2 inputs, but error rises roughly linearly with the summed duration of the input/output mappings. However, if firing patterns reflected only a few milliseconds' input, then multi-input–multioutput mapping might result in good piecewise approximations of a large family of desired outputs. This possibility is related to the liquid-state machine (Maass et al. 2002), but differs in a significant respect. Specifically, although computations in a liquid-state machine require traces of long-past inputs, we are suggesting that a similar architecture without such traces may enable population coding of time-varying inputs without time-varying firing rates.

Population–Temporal Coding

The present results make it clear that patterns of irregular spiking, perhaps generated by recurrent circuit dynamics, can drive a wide range of time-varying activity in other cells. In this light, we propose that it is reasonable to view any circuit that produces a temporal firing pattern, regardless of whether the pattern contains variations in firing rates, as being analogous to a central pattern generator. That is, such a circuit is a versatile, intrinsic source of time-varying activity patterns (although mechanisms of pattern modulation may be different from those of classical central pattern generators).

However, the ability of neurons to exploit timing-based information may have much broader uses. One interesting possibility is that a given pattern of input to a neuron might be analogous to the neuron's preferred direction, in a multidimensional population code. For example, suppose a neuron was to receive input from a number of synfire chains (Diesmann et al. 1999; Ikegaya et al. 2004). The phase relationships among $N + 1$ chains would span an N-dimensional vector space. Every vector in this space, that is, every possible list of phases, would correspond to a certain pattern of input to the receiving neuron. As the present results demonstrate, almost any such input pattern could be transformed into almost any pattern of current. Moreover, deviations from this input pattern, either in terms of phase relationships or spike timing precision, would result in noisier current, much like deviations from preferred direction in a rate-based population code result in reduced current. An ensemble of neurons with different preferred phase relationships could support a population code over the space of phase relationships. The present results also suggest that a population code of this form could drive either a similar code in a receiving ensemble of neurons or a rate-based population code (as evident from the square-pulse example of Figure 1, in that a postsynaptic neuron would fire faster during the excitatory pulse). Further work is needed to verify that such a population code can be supported by realistic neuron models and to explore its computational power.

In conclusion, the results of this study suggest that neurons can use information contained in the timing of incoming spikes, under very general conditions. Synchrony is not needed, and specialized synapses, neurons, and circuit structures are also unnecessary. Furthermore, incoming patterns can consist mostly of noise and can therefore be very hard to detect experimentally, yet still produce behaviorally useful patterns. Finally, timing-based information can be transformed into a wide variety of outputs, in a manner that seems to accommodate a versatile population code.

Notes

Address correspondence to Chris Eliasmith, HH 331, University of Waterloo, Waterloo, Ontario, Canada N2L 3G1. Email: celiasmith@uwaterloo.ca.

Appendix: Details of Power Analyses

The effect sizes for power analyses were derived from the smallest increases in the firing rates of a noisy excitatory population that could be expected to produce a spike in a cell postsynaptic to this population. For simplicity, it was assumed that PSCs would decay such that the postsynaptic cell would fire if it received more than a fixed number of spikes from excitatory sources within a 5-ms time bin. The rates of extra

spikes and missing spikes in the postsynaptic cell were assumed to be the same, so that noise could be expressed as a single index, corresponding to the rate of mistimed spikes. For each spike in a postsynaptic cell, let n be the number of excitatory neurons converging onto the postsynaptic cell that have a slightly elevated, noisy rate increase that contributes probabilistically to the spike. The mean number of spikes in each bin, across these neurons, will be different for each trial. For large n, these trial means cluster around grand means in a Gaussian distribution with variance λ/n (where λ is the Poisson spike rate per bin). Reliability of postsynaptic spiking in this scenario will increase with greater differences between the grand means of the normal and elevated rates of presynaptic spiking. The grand-mean elevated rate of presynaptic spiking was set such that trial means for each bin crossed an intermediate threshold at a rate corresponding to a predetermined rate of mistimed postsynaptic spikes. Because rates were elevated only in very short (5 ms) bins, this rate modulation can also be viewed as a noisy manipulation of spike timing.

These analyses result in estimations of the numbers of trials in various conditions, which provide a 0.8 probability of finding minimal rate elevations (if they exist), with a 1-way fixed-effects analysis of variance (ANOVA). The baseline and elevated rates were similar, so (because variance equals mean in a Poisson process) the ANOVA assumption of uniform variances was approximately satisfied. However, because the ANOVA relies on the sampling distribution of variances, which is sensitive to deviations from normality in the underlying distributions, results are presented from numerical experiments rather than from theoretical distributions. Each reported data point corresponds to the number of trials (rounded to the nearest integer) in each of a set of 1000 experiments, in which the null hypothesis (i.e., the hypothesis that there was no difference in firing rates across bins) was rejected between 799 and 801 times ($\alpha = 0.05$). The validity of the ANOVA with Poisson-distributed data in these circumstances was also confirmed, in that the null hypothesis was rejected at the $\alpha = 0.05$ level in roughly 50 of 1000 experiments in which there were no systematic rate differences, regardless of the number of trials in each experiment.

References

Abbott LF, Dayan P. 1999. The effect of correlated variability on the accuracy of a population code. Neural Comput. 11:91–101.

Abeles M. 1982. Role of the cortical neuron: integrator or coincidence detector? Isr J Med Sci. 18:83–92.

Abeles M, Bergman H, Margalit E, Vaadia E. 1993. Spatiotemporal firing patterns in the frontal cortex of behaving monkeys. J Neurophysiol. 70:1629–1638.

Ahissar E. 1998. Temporal-code to rate-code conversion by neuronal phase-locked loops. Neural Comput. 10:597–650.

Bair W, Koch C. 1996. Temporal precision of spike trains in extrastriate cortex of the behaving macaque monkey. Neural Comput. 8:1185–1202.

Benucci A, Verschure PFMJ, König P. 2004. Two-state membrane potential fluctuations driven by weak pairwise correlations. Neural Comput. 16:2351–2378.

Brand A, Behrend O, Marquardt T, McAlpine D, Grothe B. 2002. Precise inhibition is essential for microsecond interaural time difference coding. Nature. 417:543–547.

Brody CD, Hopfield JJ. 2003. Simple networks for spike-timing-based computation, with application to olfactory processing. Neuron. 37:843–852.

Buonomano DV. 2000. Decoding temporal information: a model based on short-term synaptic plasticity. J Neurosci. 20:1129–1141.

Cassidy M, Mazzone P, Oliviero A, Insola A, Tonali P, Di Lazzaro V, Brown P. 2002. Movement-related changes in synchronization in the human basal ganglia. Brain. 125:1235–1246.

Courtemanche R, Fujii N, Graybiel AM. 2003. Synchronous, focally modulated β-band oscillations characterize local field potential activity in the striatum of awake behaving monkeys. J Neurosci. 23:11741–11752.

Crick F. 1984. Function of the thalamic reticular complex: the searchlight hypothesis. Proc Natl Acad Sci USA. 81:4586–4590.

Dakin SC, Bex PJ. 2002. Role of synchrony in contour binding: some transient doubts sustained. J Opt Soc Am. 19:678–686.

Dan Y, Poo MM. 2004. Spike timing-dependent plasticity of neural circuits. Neuron. 44:23–30.

DeBusk BC, DeBruyn EJ, Snider RK, Kabara JF, Bonds AB. 1997. Stimulus-dependent modulation of spike burst length in cat striate cortical cells. J Neurophysiol. 78:199–213.

Destexhe A, Mainen ZF, Sejnowski TJ. 1998. Kinetic models of synaptic transmission. In: Koch C, Segev I, editors. Methods in neuronal modeling. 2nd ed. Cambridge (MA): MIT Press. p. 1–25.

Diesmann M, Gewaltig MO, Aertsen A. 1999. Stable propagation of synchronous spiking in cortical neural networks. Nature. 402:529–533.

Eliasmith C, Anderson CH. 2003. Neural engineering: computation, representation, and dynamics in neurobiological systems. Cambridge (MA): MIT Press.

Gütig R, Sompolinsky H. 2006. The tempotron: a neuron that learns spike timing-based decisions. Nat Neurosci. 9:420–428.

Hahnloser RHR, Kozhevnikov AA, Fee MS. 2002. An ultra-sparse code underlies the generation of neural sequences in a songbird. Nature. 419:65–70.

Hopfield JJ. 1995. Pattern recognition computation using action potential timing for stimulus representation. Nature. 376:33–36.

Ikegaya Y, Aaron G, Cossart R, Aronov D, Lampl I, Ferster D, Yuste R. 2004. Synfire chains and cortical songs: temporal modules of cortical activity. Science. 304:559–564.

Izhikevich EM. 2003. Simple model of spiking neurons. IEEE Trans Neural Netw. 14:1569–1572.

Izhikevich EM. 2006. Polychronization: computation with spikes. Neural Comput. 18:245–282.

Izhikevich EM, Desai NS, Walcott EC, Hoppensteadt FC. 2003. Bursts as a unit of neural information: selective communication via resonance. Trends Neurosci. 26:161–167.

Johansson RS, Birznieks I. 2004. First spikes in ensembles of human tactile afferents code complex spatial fingertip events. Nat Neurosci. 7:170–177.

Kepecs A, Lisman J. 2003. Information encoding and computation with spikes and bursts. Network: Comput Neural Syst. 14:103–118.

Kepecs A, van Rossum MCW, Song S, Tegner J. 2002. Spike-timing-dependent plasticity: common themes and divergent vistas. Biol Cybern. 87:446–458.

Knüsel P, Wyss R, König P, Verschure PFMJ. 2004. Decoding a temporal population code. Neural Comput. 16:2079–2100.

Koch C. 1999. Biophysics of computation. Oxford: Oxford University Press.

Kühn AA, Williams D, Kupsch A, Limousin P, Hariz M, Schneider G-H, Yarrow K, Brown P. 2004. Event-related beta desynchronization in human subthalamic nucleus correlates with motor performance. Brain. 127:735–746.

Legenstein R, Naeger C, Maass W. 2005. What can a neuron learn with spike-timing-dependent plasticity? Neural Comput. 17:2337–2382.

Levy R, Ashby P, Hutchison WD, Lang AE, Lozano AM, Dostrovsky JO. 2002. Dependence of subthalamic nucleus oscillations on movement and dopamine in Parkinson's disease. Brain. 125:1196–1209.

Lisman JE. 1997. Bursts as units of neural information: making unreliable synapses reliable. Trends Neurosci. 20:38–43.

Maass W, Natschläger T, Markram H. 2002. Real-time computing without stable states: a new framework for neural computation based on perturbations. Neural Comput. 14:2531–2560.

MacKay WA. 1997. Synchronized neuronal oscillations and their role in motor processes. Trends Cogn Sci. 1:176–183.

MacLeod K, Bäcker A, Laurent G. 1998. Who reads temporal information contained across synchronized and oscillatory spike trains? Nature. 395:693–698.

Magee JC. 1999. Dendritic Ih normalizes temporal summation in hippocampal CA1 neurons. Nat Neurosci. 2:508–514.

Magee JC, Cook EP. 2000. Somatic EPSP amplitude is independent of synapse location in hippocampal pyramidal neurons. Nat Neurosci. 3:895–903.

Medina JF, Garcia KS, Nores WL, Taylor NM, Mauk MD. 2000. Timing mechanisms in the cerebellum: testing predictions of a large-scale computer simulation. J Neurosci. 20:5516–5525.

Natschläger T, Maass W. 2001. Computing the optimally fitted spike train for a synapse. Neural Comput. 13:2477–2494.

Natschläger T, Ruf B. 1998. Spatial and temporal pattern analysis via spiking neurons. Network: Comput Neural Syst. 9:319-332.

Olney SJ, Winter DA. 1985. Predictions of knee and ankle moments of force in walking from EMG and kinematic data. J Biomech. 18:9-20.

Optican LM, Richmond BJ. 1987. Temporal encoding of two-dimensional patterns by single units in primate inferior temporal cortex. III. Information theoretic analysis. J Neurophysiol. 57:162-178.

Pellerin JP, Lamarre Y. 1997. Local field potential oscillations in primate cerebellar cortex during voluntary movement. J Neurophysiol. 78:3502-3507.

Poirazi P, Brannon T, Mel BW. 2003. Arithmetic of subthreshold synaptic summation in a model CA1 pyramidal cell. Neuron. 37:977-987.

Reinagel P, Godwin D, Sherman SM, Koch C. 1999. Encoding of visual information by LGN bursts. J Neurophysiol. 81:2558-2569.

Reinagel P, Reid RC. 2002. Precise firing events are conserved across neurons. J Neurosci. 22:6837-6841.

Riehle A, Grün S, Diesmann M, Aertsen A. 1997. Spike synchronization and rate modulation differentially involved in motor cortical function. Science. 278:1950-1953.

Rieke F, Warland D, de Ruyter van Steveninck R, Bialek W. 1997. Spikes: exploring the neural code. Cambridge (MA): MIT Press.

Rudolph M, Destexhe A. 2003. A fast-conducting, stochastic integrative mode for neocortical neurons in vivo. J Neurosci. 23:2466-2476.

Salinas E, Sejnowski TJ. 2000. Impact of correlated synaptic input on output firing rate and variability in simple neuronal models. J Neurosci. 20:6193-6209.

Schneidman E, Bialek W, Berry MJ. 2003. Synergy, redundancy, and independence in population codes. J Neurosci. 23:11539-11553.

Segundo JP, Moore GP, Stensaas LJ, Bullock TH. 1963. Sensitivity of neurones in Aplysia to temporal pattern of arriving impulses. J Exp Biol. 40:643-667.

Shadlen MN, Movshon JA. 1999. Synchrony unbound: a critical evaluation of the temporal binding hypothesis. Neuron. 24:67-77.

Singer W. 1999. Time as coding space? Curr Opin Neurobiol. 9:189-194.

Softky WR, Koch C. 1993. The highly irregular firing of cortical cells is inconsistent with temporal integration of random EPSPs. J Neurosci. 13:334-350.

Thorpe S, Delorme A, van Rullen R. 2001. Spike-based strategies for rapid processing. Neural Netw. 14:715-725.

Tomita M, Eggermont JJ. 2005. Cross-correlation and joint spectro-temporal receptive field properties in auditory cortex. J Neurophysiol. 93:378-392.

Tripp B, Eliasmith C. 2006. Comparison of neural circuits that estimate temporal derivatives. Cosyne 2006. [abstracts 196].

Williams SR, Stuart GJ. 2000. Site independence of EPSP time course is mediated by dendritic Ih in neocortical pyramidal neurons. J Neurophysiol. 83:3177-3182.

Wright BD, Sen K, Bialek W, Doupe AJ. 2002. Spike timing and the coding of naturalistic sounds in a central auditory area of songbirds. arXiv:physics 0201027.

Yin TCT, Chan JCM. 1990. Interaural time sensitivity in medial superior olive of cat. J Neurophysiol. 64:465-488.